This article was published in Separation and Purification Technology, 141, 235-245, 2015
http://dx.doi.org/10.1016/j.seppur.2014.11.046

Heterogeneous Fenton's Oxidation using Fe/ZSM-5 as Catalyst in a Continuous Stirred Tank Reactor

Samuel Queirós[1], V. Morais[1], Carmen S.D. Rodrigues[1], F.J. Maldonado-Hódar[2], Luis M. Madeira[1,*]

[1] LEPABE – Laboratório de Engenharia de Processos, Ambiente, Biotecnologia e Energia, Departamento de Engenharia Química, Faculdade de Engenharia, Universidade do Porto, R. Dr. Roberto Frias, 4200-465 Porto, Portugal

[2] Department of Inorganic Chemistry, Faculty of Sciences, University of Granada, Avenida de Fuente Nueva, 18071 Granada, Spain

* Corresponding author. E-mail address: mmadeira@fe.up.pt (Luis M. Madeira).
Tel: + 351 22 508 1519; Fax: +351 22 508 1449

Abstract

This work is the first known report dealing with the heterogeneous Fenton-like process in a continuous stirred tank reactor. A Fe/ZSM-5 zeolite was used as catalyst for degradation of an azo dye (Orange II, OII)-containing solution.

A parametric study was carried out to evaluate the effect of the main operating conditions in the basket reactor performance, namely temperature (in the range 10 – 70 ºC), pH (1.5 – 4.0), feed hydrogen peroxide concentration – $[H_2O_2]_{feed}$ (1.75 – 20.0 mM), contact time – W/Q (10 – 200 mg.min/mL), residence time – t_{resid} (30 – 180 min) and the size of the catalyst particles ($0.25< dp_1 < 0.60$, $0.60 < dp_2 < 0.80$ mm and as pellets, $dp_3 > 5$ mm), for a OII feed concentration of 0.1 mM. Under the best operating conditions found (pH = 3.0, T = 70 ºC, $[H_2O_2]_{feed}$ = 6 mM, W/Q = 200 mg.min/mL, dp_2 and t_{resid} = 90 min), it was achieved 91% of discoloration and 36% of mineralization, at steady-state. Moreover, it was found a removal of 29% in terms of the chemical oxygen demand (COD), being worth noting the improvement in the effluent biodegradability (k' – oxygen uptake rate – increased from 9.3 to 23.2 $mgO_2/(g_{VSS}.h)$) and the fact that the final effluent is non-toxic (0.0% of *Vibrio fischeri* inhibition).

The stability of the catalyst performance was checked during five consecutive runs. The crucial factor for the catalyst long-term use is the leaching of iron, which in all runs reached very low levels (e.g. only 0.173 mg/L of iron for the run in the optimized conditions, corresponding to only 0.13% of leaching). The catalyst was characterized by different techniques before and after the reactions (namely SEM/EDS and N_2 adsorption); textural and chemical transformations during its use can be considered negligible (except for very acidic conditions of pH = 1.5) favoring the catalytic stability of the Fe-zeolite.

Keywords: Continuous Stirred Tank Reactor; Heterogeneous Fenton's oxidation; Fe-Zeolite; Dye.

1. Introduction

Water pollution, caused by the discharge of effluents into the environment without prior treatment, is a serious problem worldwide. The chemical industry is one of the biggest polluting entities, where the industry of organic dyes is a non-negligible part contributing to the total pollution by ca. 3-4% [1]. It is estimated that for every ton of dyes used are produced between 25 to 250 m^3 of dye-containing effluents [2].

In textiles manufacturing, a large amount of dyes is lost during the dyeing step, because the fixation rate is sometimes only as low as 50% [3]. Thus, high volumes of colored effluents are generated, which are often difficult to degrade, although typically they contain low concentrations of dyes (approximately 0.1 mM) [4]. These compounds, and due to their complex structure, can hardly be removed by biological or physical-chemical processes such as coagulation / flocculation, sedimentation, flotation, filtration and adsorption. Moreover, in most of such processes there is only transfer of the dyes from one phase to another, rather than their destruction [5].

In recent decades, the advanced oxidation processes (AOPs) have gained importance in this area, namely the Fenton's process due to its effectiveness in degrading organic compounds at room temperature and atmospheric pressure [6]. AOPs are based on the high oxidation power of the hydroxyl radicals ($HO^{\bullet}$) generated, as compared to other existing oxidants, being capable of oxidizing most organic compounds, sometimes with total mineralization, that is, with complete oxidation until the final products as CO_2 and H_2O.

The Fenton's process is an AOP based on a catalytic reaction involving hydrogen peroxide where there is an exchange of electrons between the oxidant and a transition metal, usually iron, which acts as a catalyst, to yield, among other products, the said hydroxyl radicals, as described by the simplified equations (1) to (3) [7]:

$$Fe^{2+} + H_2O_2 \rightarrow Fe^{3+} + HO^- + HO^{\bullet} \quad (1)$$

$$Fe^{3+} + H_2O_2 \rightarrow Fe^{2+} + HO_2^{\bullet} + H^+ \quad (2)$$

$$HO^{\bullet} + \text{organic} \quad \text{matter} \rightarrow \text{oxidation} \quad \text{products} \tag{3}$$

Despite its proven efficacy, the homogeneous Fenton process has some disadvantages, including the need for a high amount of iron ions (about 50 - 80 ppm) in solution, which subsequently implies downstream processes for their removal/recovery. This removal requires the inclusion of another stage in the treatment process, thus making it more expensive and complex [7]. To minimize these disadvantages, different forms to attach the iron species to a porous solid matrix (such as a zeolite, clay or activated carbon support) were studied – so-called heterogeneous Fenton-like process [5, 8, 9-15].

The principles of the heterogeneous Fenton-like reaction are the same of the homogeneous one, however, owing to the phenomena of adsorption and catalysis, the process becomes more complex. Equations (4) and (5) present the main reactions involved:

$$X - Fe^{3+} + H_2O_2 \rightarrow X - Fe^{2+} + HO_2^{\bullet} + H^+ \tag{4}$$

$$X - Fe^{2+} + H_2O_2 \rightarrow X - Fe^{3+} + OH^- + HO^{\bullet} \tag{5}$$

where X represents the surface of the catalyst; reaction (4) describes the reduction of Fe^{3+} to Fe^{2+} yielding $HO_2^{\bullet}$ radicals (which are less oxidative than $HO^{\bullet}$ species), and then the resultant Fe^{2+} is responsible for the production of hydroxyl radicals, described in equation (5) [7].

Zeolites are hydrated aluminosilicates that can accommodate a variety of different positive ions such as iron, sodium, calcium, barium or potassium. They have a highly regular three-dimensional structure, with high porosity and, consequently, high surface area [16, 17]. Zeolites are of particular interest as catalysts in this topic; in fact, their catalytic and adsorptive potential are well known in various reactions such as the reduction of nitrous oxides, oxidation of benzene to phenol, as well as in heterogeneous AOPs, namely ozonation [18, 19], photo-Fenton [20-22] and Fenton [17, 23-26] processes.

It should be noted that the overwhelming majority of the works that are available in the literature make use of closed (or batch) reactors, which brings disadvantages of industrial applicability because they operate discontinuously. In the field of continuous packed-bed reactors, the work by Mesquita et al. [14] and Duarte et al. [8] proved the ability of iron-

containing activated carbon to act as heterogeneous catalyst in the Fenton's process. In particular, Duarte et al. [8] achieved 97% of dye degradation and 74% of total organic carbon (TOC) removal from an effluent containing 0.01 mM of alcian blue dye, while Mesquita et al. [14], for a 0.01 mM solution of chicago blue, reached removals of 88% and 47% for dye and TOC, respectively. Although there are some (but little) studies with packed-bed (or column) reactors, these reactors present problems of mass transfer due to the formation of bubbles (O_2 and/or CO_2) that are caught in the catalyst particles; such problems should not occur in a configuration like a continuous stirred tank reactor (CSTR).

The CSTR is a configuration widely used in the chemical and biological industry. Recently, it was investigated the applicability of the homogeneous Fenton process in a CSTR, where a detailed parametric study was carried out, resulting in a very good degradation of the dye, which reached 95%, proving that the concept of applying a homogeneous Fenton CSTR is plausible [27]. Other authors achieved high performances (97% for organic matter and 99% for phenolic compounds removal) when treating an olive-oil mill wastewater by the homogeneous Fenton's process using a CSTR [28]. Zhang et al. [29] applied the homogeneous Fenton oxidation in a CSTR for treating a landfill leachate effluent and also reached good efficiencies of COD removal (in the range 76.6 to 94.3% when initial COD varied between 1000 to 3000 mg/L).

The industrial wastewater processing using batch vessels (closed reactors) by the homogeneous Fenton's reagent implies a further separation of the iron in solution, presenting itself as a time consuming and with little future alternative; indeed, a secondary treatment of the effluent is required. The application of the treatment process in a heterogeneous CSTR presents itself as a promising approach, allowing operating continuously and without the disadvantages of the homogeneous process. Moreover, and up to the author's knowledge, it was never tested before. In this work it is therefore intended to proof the concept of applying the Fenton's process in a continuous heterogeneous perfectly stirred tank reactor, and evaluate the influence of some parameters on the degradation of the dye Orange II (OII).

2. Materials and Methods

2.1 Catalyst and its Characterization

The catalyst selected for this work was a zeolite in pellets form (d_p > 5 mm), with trade name Alsi-Penta Fe/ZSM-5 (ref. FE-SH-27). These pellets were milled and sieved to obtain different fractions (0.25< dp_1 < 0.60, 0.60 < dp_2 < 0.80 mm and as pellets, dp_3 > 5 mm). The fresh and used zeolite samples were morphologically characterized by scanning electron microscopy (SEM) using a GEMINI (Carl Zeiss SMT) microscope equipped with EDS microanalysis; the iron distribution was analyzed by mapping before and after the catalytic reactions.

The porous texture of the materials was analyzed by N_2 adsorption at −196 ºC using an Autosorb 1 equipment from Quantachrome. Prior to measuring the N_2 adsorption isotherms, samples were outgassed overnight at 110 ºC and under high vacuum (10^{-6} mbar). N_2 adsorption isotherms were analyzed by the BET equation (bellow P/P_0 = 0.10) from which the surface area, S_{BET}, was obtained. To characterize the microporosity of the samples, the Dubinin–Radushkevich (DR) equation was applied to N_2 adsorption data [30]:

$$W = W_0 \exp\left[\left(-\frac{A}{\beta E_0}\right)^2\right] \tag{6}$$

where W is the amount adsorbed at relative pressure P/P_0, W_0 is the limiting value filling the micropores (micropore volume), A is the differential molar work given by $A = RT \ln(P_0/P)$, β is the affinity coefficient, taken to be 0.33 for N_2, and E_0 is the characteristic adsorption energy. Then the mean micropore width, L_0, was obtained by applying the Stoeckli equation [31]:

$$L_0\ (\text{nm}) = \frac{10.8}{E_0\left(\frac{\text{kJ}}{\text{mol}}\right) - 11.4} \tag{7}$$

The pore size distributions (PSD) were determined by applying the Quenched Solid Density Functional Theory (QSDFT), assuming slit-shaped pores and BJH derived methods [32, 33] to the N_2 adsorption isotherms. The total pore volume is considered as the volume of adsorbed nitrogen at a relative pressure of P/P_0 = 0.95 ($V_{0.95}$) according to Gurvitch's rule. Thus, mesopore volume, V_{meso}, was obtained from the difference between the total pore volume ($V_{0.95}$) and the micropore volume (W_0 (N_2)) [34].

The X-ray photoelectron spectra (XPS) were obtained by a Kratos Axis Ultra HAS apparatus, with VISION software for data acquisition and CASAXPS software for data analysis. The analysis was carried out with a monochromatic Al Kα (1486.7 eV) X-ray source operating at 15 kV (90 W), in FAT mode (Fixed Analyzer Transmission), with a pass energy of 40 eV for regions ROI and 80 eV for survey. Data acquisition was performed with a pressure lower than 1×10^{-6} Pa, and it was used a charge neutralization system. The binding energy of C1s peak at 285 eV was taken as a reference. The deconvolution of spectra was carried out using the CasaXPS program, in which the peak fitting was performed using Gaussian-Lorentzian peak shape and Shirley type background subtraction.

2.2 Heterogeneous Fenton Experiments

The dye Orange II was the model compound used in this study, whose chemical formula is $C_{16}H_{11}N_2NaO_4S$ and molar mass 350.33 g/mol. Orange II is one of the most widely used dyes for textiles, food, cosmetics, etc.

The experiments were conducted in an acrylic jacketed reactor (0.92 L of capacity) coupled to a thermostatic bath (Huber Polystat CC2) so as to control the temperature inside the vessel. Figure S.1 (of the supporting information section) shows a schematic of the setup used in this work. The reactor was equipped with a magnetic stirrer (VWR VS-C7) allowing maintaining a high degree of agitation (200 rpm) and a pH meter (WTW - inoLab pH 730) equipped with a temperature and pH electrode (WTW-SenTix 81) so as to make a continuous monitoring of these parameters.

The reactants were immersed in the thermostatic bath and were pumped into the reactor using a Gilson M312 peristaltic pump, with adjustment of rotation speed, through two separate streams: one containing the H_2O_2 solution, the other containing the dye solution; at the inlet of the reactor the OII solution had a concentration of 0.1 mM. Both solutions had a pH previously adjusted to that of the test, which was done using a 1 M sulfuric acid solution. Inside the continuous stirred tank reactor, a given amount of the zeolite catalyst was immersed, placed inside a porous support.

The outlet stream of the reactor, i.e. the treated effluent, was analyzed on-line through a Helios Gamma spectrophotometer from Unicam (model 9423 UVG 1002E), equipped with a flow-through cell, which was set to read at λ_{max} = 486 nm – characteristic wavelength of the used dye. Samples of such effluent were collected for further analysis of total organic carbon and iron content, as detailed below. To these samples it was added sodium sulfite in excess to stop the homogeneous reaction between remaining hydrogen peroxide and any leached iron.

2.3 Analytical Methods

In all oxidation experiments, samples were regularly taken for total organic carbon analysis (TOC) and to determine the iron leached out from the zeolite support. TOC (difference between total carbon – TC – and inorganic carbon – IC) was measured in a Shimadzu TOC-5000A (Method 5310 D) [35] apparatus; all TOC values reported are the average of at least two TC and IC measurements with a CV (coefficient of variation) < 2%. For the iron leaching quantification, the iron in solution was measured by flame atomic absorption spectrometry - Method 3111 B [35] - using an AAS UNICAM spectrophotometer (model 939/959).

The biodegradability of the effluents was evaluated by measuring the specific oxygen uptake rate (k) at 20 ºC [35, 36]. The samples were inoculated with biomass from the activated sludge tank of a WWTP processing textile effluents, and the dissolved oxygen (DO) concentration measured for 30 min (using a YSI Model 5300 B biological oxygen monitor), a period necessary to reach a DO value close to 1 mg/L. The specific oxygen uptake rate (k') was calculated as the ratio between the oxygen concentration decay rate (which was linear in the above-mentioned period) and the volatile suspended solids (VSS) concentration after the addition of the inoculum (725 mg VSS/L).

The inhibition of *Vibrio fischeri* test was performed according to the standard DIN/EN/ISO 11348-3 [37]. The bacterium was put in contact with samples at 15 ºC and the bioluminescence measured after a contact time of 5, 15 or 30 minutes in a Microtox model 500 analyzer.

The chemical oxygen demand (COD) was determined by the acidic digestion (closed reflux) method at 150 ºC for 2 h (Thermoreactor TR 300 from Merck), using potassium dichromate as

oxidant, followed by measuring the absorbance (Spectroquant Nova 60) corresponding to the reduced chromium – Method 5220 D [35].

3. Results and Discussion

3.1. Catalyst Characterization

ZSM-5 (Zeolite Socony Mobil–5) zeolite was first synthesized by Argauer and Landolt and Patented by the Mobil Oil Company in 1972 [38]. Belonging to the pentasil family of zeolites, it is a medium pore zeolite with channels defined by ten-membered rings. The estimated pore size of the channel is 5.4–5.6 Å and the total pore volume 0.242 cm^3g^{-1} [39]. In this case, we have been using the commercial Alsi-Penta Fe/ZSM-5 zeolite (ref. FE-SH-27) as catalyst. The textural characteristics of this material are summarized in Table 1. As observed, fresh Fe/ZSM-5 catalyst presents a micropore width (L_0) and a total pore volume (V_T) that are quite similar to those previously described for pure ZSM-5. When this catalyst is used in Fenton-like reactions (described in section 3.2), two simultaneous effects can modify the original pore texture: (i) due to the acidic conditions used along the experiments, metal leaching can occur, which should increase both the pore diameter and pore volume, and (ii) the formation of permanently adsorbed species on the catalyst surface, blocking in this case the porosity. When comparing the results of fresh and used catalysts one can deduce that process (i) is progressively favored with decreasing pH values, according to the evolution of L_0 (Table 1); however, V_T does not increase, but on the contrary, clearly decreases in this sense. Thus, the stronger differences of BET surface area values and micropore volumes observed for fresh and used catalysts correspond to the sample used at pH= 1.5. This means that Fe-leaching can develop certain enlargement of the zeolite porosity, but that during reaction some organic molecules can remain permanently adsorbed on the catalyst surface blocking some of these pores. Both factors seem to be favored with decreasing pH. Figure 1a shows the smaller adsorption capacity of the sample used at pH=1.5 and a good correspondence of N_2-adsorption isotherms of the rest of the samples. Also, Figure 1b points out that the pore size distribution (PSD) obtained by application of the DFT theory to the N_2-adsorption isotherms is maintained after the catalytic experiments. As observed, all samples (fresh and used) present porosity in a similar range, i.e. the position of the maxima observed (at 3.3, 4.5 and 8.8 nm) are maintained, which

seem to indicate that no significant transformations occur during reaction, except if very acidic conditions are employed.

For all samples (fresh and used at different pH values) the XPS results evidenced that the valence state of Fe in the zeolite surface is 3+ (data not shown for brevity reasons). This is due to presence of Fe_2O_3 species in fresh zeolite (in accordance with reported information for this catalyst [17, 40, 41]) and Fe(OH)O species in the zeolite after being used in oxidation runs at different pH values.

Looking for some further information, samples were also characterized by SEM and their composition analyzed by EDS in order to evaluate the possible Fe-leaching. Figure 2 shows that the catalyst is formed by amorphous particles several hundred of micrometers long (Fig 2a), while more detailed micrographs show that the surface morphology of these particles did not significantly changed after reaction (Figures 2b and c). When analyzing the composition and the distribution of the metallic elements on the catalyst surface (Figure 3), it was also observed that the surface iron content and distribution remains constant after reaction, except for very low pH values (1.5). The iron content (in an oxide base, i.e. as Fe_2O_3) is, for the fresh sample (Fig. 3a), around 9%, which corresponds to 6.0 wt.% of Fe; for the other samples iron content is similar (data not shown) while for the one used at pH 1.5 there is a decrease to 5.5 wt.% of Fe (9.3% as Fe(OH)O). This is a consequence of the iron leaching, as detailed below.

Concluding, textural, morphological and surface chemistry characterization seems to point out that the catalyst basically remains stable after reactions in severe conditions (except if pH is decreased down to 1.5), as detailed in the following sections.

3.2. Catalytic Tests

3.2.1 Stability of the catalyst

The loss of activity of a Fenton-like catalyst may be due to different phenomena such as iron leaching, pore blocking, etc. As the number of runs and change of experimental conditions

would imply the stop and restart of the reactor, charging every time with fresh catalyst, five consecutive tests were performed, under the same and typical operating conditions (pH = 3, $0.60 < d_p < 0.80$ mm, T = 50 ^{o}C, $[H_2O_2]_{feed}$ = 6 mM, W/Q = 60 mg.min/mL and t_{resid} = 30 min), to assess whether loss of activity would occur or not. It was observed a maximum variation of only 6 % in discoloration after steady-state has been reached (Figures S.2 and 4 a) and of 3% for TOC removal (Figure 4 a) among the different experiments. In the first run it was reached 69 and 21% of color and TOC removal, respectively, while in the last run the respective performances were 65 and 20%. However, as mentioned, the differences in the performances for the 5 consecutive runs are small, and within analytical uncertainty of the methods, thus corroborating catalyst stability.

The leached iron in all runs was stable and <0.3 mg/L (see Figure 4 b), which is far below the legal limits (2 mg/L).

Results obtained allowed concluding that the zeolite catalyst is stable, as reported in similar studies [5], or even more stable. In fact, Idel-aouada et al. [26] observed a little decrease of acid red 14 dye reduction (from 100 to 93% in the 1st vs. 3rd run, respectively) when using a Fe(II)-Y zeolite as catalyst, while other authors noticed some decay of activity with other supports like saponite clay [9]; activated carbons also proved to be stable [8, 14].

To assess whether the contribution of homogeneous oxidation due to the leached iron has or not significant influence on the overall process, a new experiment was performed in which the same concentration of iron that leached out from the Fe/ZSM5 zeolite was fed to the reactor. Thus, the same operating conditions as when the Fe/ZSM-5 was used were employed, only substituting the zeolite catalyst by dissolved ferrous sulfate (using in the reactor feed an Fe^{2+} dose of 0.262 mg/L – cf. Fig. 4b)) – this way oxidation is due only due to the homogeneous process. The dye outlet concentration throughout the reaction time is presented in Figure S.3 for both runs (homogeneous and heterogeneous), while the dye and TOC removal at steady state are shown in Figure 5. It can be concluded that the contribution of the homogeneous Fenton-like process is very small because only 9% of dye removal and 3% of TOC reduction were reached, compared to 69 and 21% when the zeolite was employed, respectively.

Afterwards, a parametric study was carried out for evaluating the effect of various operating conditions, namely pH, diameter of catalyst particles, temperature, feed hydrogen peroxide

concentration, contact time and residence time, in the dye degradation (color and TOC removal) and iron leached out from the support.

3.2.2. Influence of the dose of H_2O_2 in the CSTR feed

Concerning the hydrogen peroxide concentration, it is worth mentioning that to mineralize (or oxidize up to CO_2) 1 mole of OII, 42 moles of H_2O_2 are required ($C_{16}H_{11}N_2NaO_4S + 42\ H_2O_2 \rightarrow 16\ CO_2 + 46\ H_2O + 2\ HNO_3 + NaHSO_4$) [42]. Because hydrogen peroxide is also consumed in side reactions that do not produce hydroxyl radicals, the amount of oxidant required is generally higher than the stoichiometric dose. So, for a 0.1 mM solution of OII at the inlet of the reactor, concentrations of hydrogen peroxide ranging from 1.75 to 20 mM were employed (corresponding to 0.42 – 4.76 of the stoichiometric dose). As shown in Figure S.4, where again the results obtained in terms of the dye dimensionless concentration at the outlet of the reactor are presented, and in Figure 6 a (at steady-state for both the dye and TOC removal as a function of the feed H_2O_2 concentration), it was observed an optimum performance for the dose of 6 mM (corresponding to a stoichiometric dose of 1.42). For an oxidant concentration below the stoichiometric dose it was expected that the discoloration was smaller, which was really observed; for concentrations well above the stoichiometric dose (10 mM - 20 mM), excess oxidant is consumed in scavenging reactions ($H_2O_2 + HO^{\bullet} \rightarrow HO_2^{\bullet} + H_2O$), thus implying that the hydroxyl radicals are not available at concentrations high enough to proceed with organics oxidation. In fact, the radical formed ($HO_2^{\bullet}$) has an oxidation potential that is lower than the hydroxyl radical one, which explains the decrease in performance. These results are in agreement with previous works (e.g. Santos et al. [43]).

For the optimum oxidant dose of 6 mM, it was reached 69% of color removal and 21% of TOC removal, in steady-state (Figure 6). This optimum dose is equal to the one found by Ramirez et al. [9] for treating the same dye, in batch mode, using saponite clay and activated carbon catalysts impregnated with iron. It is also similar to that reported in other studies [13, 26, 44].

Concerning the iron concentration in the outlet effluent, it was not observed any clear relation between this parameter and the concentration of hydrogen peroxide (see Figure 6 b), as also reported by Duarte et al. [8]. It is however curious that higher leaching was found for a feed

H_2O_2 dose of 6 mM. The iron leaching in these runs varied in the range of 0.05 to 0.234 mg/L, far below the standard limit for discharge (2 mg/L).

3.2.3. Effect of catalyst particle size

To evaluate the effect of the catalyst particle size (d_p), three runs were carried out in which this parameter was changed as follows: $0.25 < dp_1 < 0.6$ mm, $0.6 < dp_2 < 0.8$ mm and in pellets form ($dp_3 > 5$ mm). In Figure 7 a it can be observed that the dye removal, upon reaching steady state, was very similar for the smaller sizes (71 and 69% for dp_1 and dp_2, respectively) and decreased considerably for the pellets – it was only reached 28% of dye removal. Results in transient regimen are shown in Figure S.5. The results of TOC removal followed the same trend of dye reduction (see Figure 7 a); it was found that TOC removal was very low for pellets (12%), while for the other two runs the removals were almost not affected by the particle size (reaching 23 and 21% for dp_1 and dp_2, respectively - differences are within analytical uncertainty). The explanation for the fact that the dye (or TOC) removal was similar for dp_1 and dp_2 is related with the absence of internal mass transfer resistances for these small particle sizes [45-48]. For small particle sizes (small Thiele modulus values) one in under chemical regime, i.e. the effectiveness factor is close to 1; so, under such conditions, and independently of the d_p value, observed reaction rate (or conversion) is the same. For larger particles, mass transfer resistances due to internal pore diffusion become significant, and the catalyst performance decays, as observed for dp_3.

The values of the iron concentration in the treated wastewater suggest that a decrease in particle size leads to increased catalyst leaching, as can be seen in Figure 7 b. This trend is in agreements with previous works, even in slurry batch reactors and with activated carbon-based catalysts, where it was found that smaller Fe particles (better dispersion) were observed for supports with smaller particle size, leading to more active catalysts but also with higher Fe leaching [34].

According to the dye and TOC removal and iron leaching results, it was selected the dp_2 (range between 0.6 to 0.8 mm) as optimal size for subsequent Fenton oxidation runs in the CSTR.

3.2.4. Influence of pH

The Fenton reaction usually occurs in acidic medium (pH 2-4), as this range of values facilitates the production of hydroxyl radicals [49]. Thus, assays were carried out at pH values between 1.5 and 4.0, as shown in Figures S.6 and 8 a, where it can be seen that at pH values around 2.0-3.0 higher color and TOC removals were reached. These optimums values of pH are similar to those obtained in studies reported in literature when treating a dye solution with Fe-zeolite Y [13] or Fe-activated carbon [8, 14] as catalyst. It was observed, as expected, a decrease in conversion with pH values greater than 3, probably due to the lower stability of hydrogen peroxide, which decomposes into molecular oxygen instead of being used for generating the radicals. Moreover, under such conditions the formation of ferrous/ferric hydroxide complexes occurs, which lead to the deactivation of the ferrous catalyst [50]; moreover, the oxidation potential of the hydroxyl radical also decreases with increasing pH (2.65–2.80 at pH = 3 and 1.90 V at pH = 7) [11]. On the other hand, the decreased efficiency of the process at very acidic pH values may be related to the decreased generation of hydroxyl radicals, once the hydrogen peroxide forms the hydroperoxonium ion ($H_3O_2^+$) by proton solvation, and therefore does not react with iron [5]. However, in terms of iron concentration in the effluent, lower pH values provide rather poor results (Figure 8 b), so that for pH = 1.5 the limit of 2 ppm of iron is exceeded, showing a great leaching of the initial iron present in the catalyst. In fact, it was not possible, at this value of pH, to obtain two consecutive reproducible trials with the same sample (low catalyst stability).

Therefore, pH = 3 seems to be the most balanced value, ensuring reasonable TOC and color removals (21 and 66%, respectively) and a low value of iron concentration in the treated effluent. A similar optimum pH was found in previous works [10, 44, 51].

Finally, it should be noted that any decrease of effluent pH, for the different pH values employed in the feed stream, were observed. Although TOC removals were not high in these runs, which could lead to formation of acidic intermediates, the fact that pH didn’t change can be related with the very small concentration of organics present in the reactor feed.

3.2.5. Effect of the residence time

Experiments were also performed to determine whether any influence of the residence time exists in the reduction of color and TOC. In homogeneous systems this parameter has a direct influence on the reaction efficiency [27]. However, for a heterogeneous reaction this should not occur, since the contact time (*W/Q* ratio) was kept constant when varying the residence time. The residence time ($\tau = \frac{V}{Q}$) was varied from 30-180 minutes for the same *W/Q* ratio (60 mg.min/mL); in other words, for a fixed reactor volume, *V*, the feed flow rate *Q* was varied between maximum and minimum values allowed in accordance with the used peristaltic pump specifications by changing in the same proportion the mass of catalyst, *W*, so that the contact time (*W/Q*) remained unchanged.

It was found, however, that when increasing the residence time discoloration and removal of TOC reached higher values, as can be seen in Figure 9 a; results in transient regime are shown in Figure S.7. These results indicate that there are other phenomena occurring simultaneously with the heterogeneous Fenton process, anticipating a possible contribution of the homogeneous reaction due to iron leaching. This is corroborated by the results obtained from the analysis of iron present in the treated effluent (Figure 9 b). It appears that the increased residence time (lower flow rate) leads to higher concentrations of dissolved iron, which explains the observed increase in the oxidation degree (Figures 9 a and b). Nevertheless, even for a long residence time (t_{resid} = 180 min), the values of iron concentration in the effluent (0.598 mg/L) were below the limit imposed by law. Subsequent runs were however carried out with a t_{resid} value of only 30 min to minimize also contribution of the homogeneous reaction. Moreover, in practice this could also decrease installation and exploitation costs because a smaller reactor would be needed (for the same feed flow rate).

3.2.6. Influence of the contact time – *W/Q*

The effect of the *W/Q* ratio was also studied, by performing assays in the range 10-200 mg.min/mL (which was defined by the physical limitations of the set-up). Results in transient regime are reported in Figure S.8, while at steady-state are shown in Figures 10 a and b. As expected, increasing the *W/Q* ratio results in an increase of the discoloration and also of the

TOC removal by virtue of the increasing contact time (i.e., the amount of catalyst available in the reactor is increased for the same feed flow rate). This increase is reflected in the rate of production of hydroxyl radicals, resulting in increased efficiency of the color removal and oxidation of organic matter. Thus, for a W/Q = 200 mg.min/mL, it was obtained, at steady state, a discoloration of 84% and a TOC removal of 26% with the catalytic CSTR.

The amount of iron present in the reactor outlet stream increased with W/Q, reaching a concentration of 0.109 mg/L in the run with W/Q = 10 mg.min/mL and 0.512 mg/mL in the run with W/Q = 200 mg.min/mL. However, these values were still smaller than legislated values for effluent discharge (2 mg/L).

3.2.7. Influence of the reaction temperature

The temperature was another of the parameters analyzed. Four runs were performed, with temperatures between 10-70 ºC, whose results are shown in Figures S.9 and 11. It can be seen that both the discoloration and mineralization increased with the reaction temperature, which is in agreement with the Arrhenius law (reflected by the effect of temperature either on the radicals generation rate constant, or on the degradation of organic molecules by these radicals). Thus, with a temperature of 70 °C it was reached a reduction of 89% on the dye concentration and the removal of TOC was 29%. In fact, this parameter was found to be the most influential one in the process, since for low values of temperature (10 °C) color conversion was below 10%, while mineralization was only 6%. These low efficiencies at 10 ºC and increased performances for temperatures between 50-70 ºC were reported in other studies that address the heterogeneous Fenton oxidation for removal of dyes and other pollutants [5, 8, 10, 14, 52].

Regarding iron leaching, in Figure 11 b it is observed that it increased with temperature but only up to 50 ºC; in fact, it remained practically constant for a higher temperature (70 ºC). The values observed in all runs were again much smaller than the legislation standard (2 mg/L).

3.2.8. Orange II dye degradation model

For orange II dye degradation in the CSTR a simplified model was elaborated, as described along this section. The mass balance in the reactor, at steady-state, yields:

$$QC_o = QC + (-r)W \tag{8}$$

where Q is the volumetric flow rate, C_0 is feed dye concentration, C is the outlet dye concentration at steady-state, $(-r)$ is the reaction rate, and W stands for the mass of catalyst. Assuming a first-order reaction kinetics ($(-r) = kC$), where k is the apparent kinetic constant, and from the definition of dye conversion:

$$C = C_0 (1 - X) \tag{9}$$

one obtains:

$$X = \frac{k \frac{W}{Q}}{1 + k \frac{W}{Q}} \tag{10}$$

Non-linear fitting of equation 10 to experimental dye conversion at different contact time values (W/Q) gives the k parameter; it was obtained a pseudo-first order kinetic constant for orange II degradation of 0.0297 mL/($mg_{catalyst}$.min). Figure 12 a) shows that the experimental and model values are very similar, i.e. the model adherence is very good.

From equation 10 and dye conversion data at different temperatures, it was possible to compute the kinetic constant at values from 10 to 70 ºC. The dependence of the obtained kinetic constants from temperature is in good agreement with the Arrhenius law (equation 11), as shown in Figure 12 b. From this linearization it was possible to determinate the value of the pre-exponential factor, k_0 (9.16×10^8 mL/($mg_{catalyst}$.min)), and the activation energy, E_a (64.5 kJ/mol) of the dye degradation by the heterogeneous Fenton process. The value of the activation energy reached is quite similar (56.1 kJ/mol) to that achieved by other authors for degradation of orange II dye by the same process but using instead Fe-C catalysts [53].

$$k = k_0 \exp\left(-\frac{E_a}{RT}\right) \tag{11}$$

The comparison between dye conversion experimental data at different temperatures and the model prediction (equation 10, using the above-mentioned k_0 and E_a values) is shown in Figure 12 c); again, the model presents a very good fit to the experimental values.

3.2.9. Treatment of Orange II dye solution – Impact in effluent biodegradability

After evaluating the effect of each operating variable on the heterogeneous Fenton process, one new experiment was carried out under the operating conditions that maximize the color and TOC removals while avoiding excessive iron leaching: $[H_2O_2]$ = 6 mM, T = 70 °C, t_{resid} = 90 min, *W/Q* ratio = 200 mg.min/mL, dp_2 (0.60 – 0.80 mm) and pH = 3.0.

The test was again run until steady-state was reached and further extended, till nearly 240 minutes, as shown in Figure S.10 of the Supporting Information section. The results of the color, TOC and COD removals at steady state were the highest of all the experiments, reaching 91, 36 and 29%, respectively. The effluent produced continued to be non-toxic, once the inhibition of *Vibrio fischeri* was 0% before and after Fenton's reaction; however, the biodegradability was considerably increased (specific oxygen uptake rate increased from 9.3 to 23 $mgO_2/(g_{VSS}.h)$ – see Figure 13).

The iron concentration in the effluent remained well below legal limits, with a final value of 0.153 mg/L, corresponding to an iron leaching from the support of only 0.13%.

4. Conclusions

This work had as main objective the operation of a continuous perfectly stirred tank reactor in order to treat a colored effluent through the heterogeneous Fenton's reagent using a zeolite as catalyst. It was also aim of this study to investigate the influence of some parameters such as temperature, oxidant concentration, pH, contact time (*W/Q* ratio), residence time and the diameter of the catalyst particles on the efficiency of the dye and TOC removal from the effluent. It was chosen as a model dye OII, due to its wide use in various fields such as textile and chemical industry.

It was proved that the parameter with the larger influence on the degradation of OII and on the removal of TOC is the temperature, which is due to the Arrhenius (exponential) dependence

of the reaction rates involved, either the generation of hydroxyl radicals, or the oxidation of organic matter, on this parameter. It was concluded that parallel homogeneous reactions, due to iron leached out from the support, are present during the heterogeneous process, as the conversion of color and the TOC removal increased with the increasing residence time; however, in certain conditions they contribution can be neglected.

The textural and chemical characterization of spent catalysts pointed out that smaller differences of BET surface area and micro and mesopore volumes were observed in fresh and used zeolite, suggesting a great stability of the catalyst, which was also experimentally observed as long as pH > 2. Indeed, catalyst stability was proven in the used basket reactor configuration after subsequent cycles. The following conditions were set as promising, within the ranges studied in the parametric study: temperature of 70 °C, hydrogen peroxide concentration of 6 mM in the feed of the reactor, pH = 3, W/Q = 200 mg.min/mL, and residence time of 90 min, which allowed to obtain, at steady state, color, TOC and COD removals of 91, 36 and 29%, respectively. A more biodegradable (k' increased from 9.3 to 23.2 $mgO_2/(g_{VSS}\,h)$) and a non-toxic (0.0% of *Vibrio fischeri* inhibition) effluent was obtained after Fenton's reaction in the catalytic CSTR. Iron concentration in the solution was 0.173 mg/L, corresponding to only 0.13% of iron leaching.

The legal limits of concentration due to leached iron (2 ppm) were only achieved in the test with pH = 1.5 (2.95 ppm), while in the remaining tests the results stood well below the limit imposed by legislation; this demonstrates the feasibility of industrial application of this process in a heterogeneous CSTR for treatment of colored effluents.

Acknowledgments

The authors are thankful to TRATAVE S.A. (WWTP of Rabada) for providing the aerobic biological sludge for the respirometric tests, to Doctor Rui Boaventura for supplying the Microtox and Respirometer apparatus for measuring the *Vibrio fischeri* inhibition and carrying out the respirometric tests, respectively, and to CEMUP for the XPS analysis. Carmen Rodrigues is grateful to FEDER/ON2 for financial support through the Postdoctoral grant (Ref. Norte-07-0124-FEDER-000025).

Appendix A. Supporting Information

Supplementary material associated with this article is available online.

References

[1] E. A. Clarke, Rev. Prog. Color. Relat. 25 (1995) 1-5.

[2] M.S. Lucas, J.A. Peres, Dyes and Pigments 74 (2007) 622-629.

[3] J.R. Easton, The dye maker's view. In Colour in Dyehouse Effluent P. Cooper (Ed.). Oxford, The Society of dyers and Colourists, The Alden Press, 1995.

[4] C.R. Corso, A.C. Almeida, Microb. Ecol. 57 (2009) 384-390.

[5] M.L. Rache, A.R. García, H.R. Zea, A.M.T. Silva, L.M. Madeira, J.H. Ramírez, Appl. Catal. B - Environ. 146 (2014) 192-200.

[6] A. Babuponnusami, K. Muthukumar, Journal of Environmental Chemical Engineering (2013) 557-572.

[7] C. Walling, Acc. Chem. Res. 8 (1975) 125-131.

[8] F. Duarte, V. Morais, F.J. Maldonado-Hódar, L.M. Madeira, Chem. Eng. J. 232 (2013) 34-41.

[9] J.H. Ramirez, C.A. Costa, L.M. Madeira, G. Mata, M.A. Vicente, M.L. Rojas-Cervantes, A.J. López-Peinado, R.M. Martín-Aranda, Appl. Catal. B – Environ. 71 (2007) 44-56.

[10] J.H. Ramirez, F.J. Maldonado-Hódar, A.F. Pérez-Cadenas, C. Moreno-Castilla, C.A. Costa, L.M Madeira, Appl. Catal. B – Environ. 75 (2007) 312-323.

[11] A. Chen, X. Ma, H. Sun, J. Hazard. Mater. 156 (2008) 568-575.

[12] F. Duarte, F.J. Maldonado-Hódar, A.F. Pérez-Cadenas, L.M. Madeira, Appl. Catal. B – Environ. 85 (2009) 139-147.

[13] H. Hassan, B.H. Hameed, Desalination 276 (2011) 45-52.

[14] I. Mesquita, L.C. Matos, F. Duarte, F.J. Maldonado-Hódar, A. Mendes, L.M. Madeira, J. Hazard. Mater. 237-238 (2012) 30-37.

[15] S. Fukuchi, R. Nishimoto, M. Fukushima, Q. Zhu, Appl. Catal. B – Environ.174 (2014) 411-419.

[16] M. Hartmann, S. Kullmanna, H. Keller, J. Mater. Chem. 20 (2010), 9002-9017.

[17] F. Duarte, L.M. Madeira, Separ. Sci. Technol. 45 (2010) 1512-1520.

[18] H. Valdés, R.F. Tardón, C.A. Zaror, Chem. Eng. J. 211-212 (2012) 388-395.

[19] A. Ikhlaq, D.R. Brown, B. Kasprzyk-Hordern, Appl. Catal. B – Environ. 154-155 (2014) 110-122.

[20] I. Grcic, M. Muzic, D. Vujevic, N. Koprivanac, Chem. Eng. J. 150 (2009) 476-484.

[21] M. Aleksić, H. Kušić, N. Koprivanac, D. Leszczynska, A.L. Božić, Desalination 257 (2010) 22-29.

[22] M.J. MacDonald, Z. Wub, J.-Y. Ruzicka, V. Golovko, D.C.W. Tsang, A.C.K. Yip, Separ. Purif. Techn. 125 (2014) 269-274.

[23] H. Kusic, N. Koprivanac, I. Selanec, Chemosphere 65 (2006) 65-73.

[24] M. Dükkanci, G. Gunduza, S. Yılmazb, R.V. Prihod'koc, J. Hazard. Mater. 181 (2010**)** 343-350.

[25] A.N. Soon, B. Hameed, Desalination 269 (2011) 1-16.

[26] R. Idel-aouada, M. Valientea, A. Yaacoubib, B. Tanoutic, M. López-Mesas, J. Hazard. Mater. 186 (2011) 745-750.

[27] J.H. Ramirez, F.M. Duarte, F.G. Martins, C.A. Costa, L.M. Madeira, Chem. Eng. J. 148 (2009) 394-404.

[28] G. Hodaifa, J.M. Ochando-Pulido, S. Rodriguez-Vives, A. Martinez-Ferez, Chem. Eng. J. 220 (2013) 117-124.

[29] H. Zhang, H.J. Choi, C.-H. Huang, J. Hazard. Mater. B136 (2006) 618–623.

[30] R.C. Bansal, J.B. Donnet, F. Stoeckli, Active Carbon, Marcel Dekker, New York, 1998.

[31] F. Stoeckli, In Porosity in Carbons. Characterization and Applications, Patrick, J. W., Ed. Edward Arnold, London, 1995.

[32] E.P. Barrett, L.G. Joyner, P.P. Halenda, J. Am. Chem. Soc. 73 (1951) 373-380.

[33] A.V. Neimark, Y. Lina, I. Peter, P.I. Ravikovitchb, M. Thommes, Carbon 47 (2009) 1617-1628.

[34] F. Duarte, F.J. Maldonado-Hódar, L.M.; Madeira, Ind. Eng. Chem. Res. 51 (2012) 9218-9226.

[35] APHA, AWWA, WEF Standard methods for the examination of water and wastewater, twentieth ed. Washington, DC: American Public Health Association, American Water Works Association, Water Pollution Control Federation, 1998.

[36] R.S. Ramalho, Introduction to wastewater treatment processes, Academic Press, New York, 1977.

[37] International Organization for Standardization. Water Quality - Determination of the Inhibitory Effect of Water Samples on the Light Emission of Vibrio Fischeri (luminescent Bacteria Test) - Part three: Method Using Freeze-dried Bacteria, 2005.

[38] R.J. Argauer, G.R. Landolt, Mobil Oil Corp. Patent US3702886 A. Crystalline zeolite zsm-5 and method of preparing the same, 1972.

[39] E.L. First, C.E. Gounaris, J. Wei, C.A. Floudas, Phys. Chem. 13 (2011) 17339-17358.

[40] R. Q. Long, R. T. Yang, J. Catal. 194 (2000) 80–90.

[41] Y. Yan, S. Jiang, H. Zhang, X. Zhang, Chem. Eng. J. 259 (2015) 243-251.

[42] J. Feng, X. Hu, P.L. Yue, Water Res. 40 (2006) 641-646.

[43] M.S. Santos, A. Alves, L.M. Madeira, Paraquat removal from water by oxidation with Fenton's reagent, Chem. Eng. J. 175 (2011) 279-290.

[44] N.K. Daud, B.H. Hameed, Desalination 269 (2011) 291-293.

[45] H.S. Fogler, Elements of Chemical Reaction Engineering, 3rd ed., Prentice Hall, New Jersey, 1999.

[46] G.F. Froment and K.B. Bischoff, Chemical Reactor Analysis and Design, 2nd ed., John Wiley & Sons, New York, 1990.

[47] O. Levenspiel, Chemical Reaction Engineering, 3rd ed., John Wiley & Sons, New York, 1999.

[48] A.E. Rodrigues, "Scientific basis for the design of two phase catalytic reactors", in Multiphase Chemical Reactors, Volume II – Design Methods, A.E. Rodrigues, J.M. Calo and N.H. Sweed (Eds.), NATO ASI Series, Sijthoff Noordhoff, 65, 1981.

[49] E. Neyens, J. Baeyens, J. Hazard. Mater. 98 (2003) 33-50.

[50] Y. Deng, J.D. Englehardt, Water Res. 40 (2006) 3683-3694.

[51] T.D. Nguyen, N.H. Phanb, M.H. Doa, K.T. Ngoa, J. Hazard. Mater. 185 (2011) 653-661.

[52] Y. Yao, L. Wang, L. Sun, S. Zhu, Z. Huang, Y. Mao, W. Lu, W. Chen, Chem. Eng. Sci. 101 (2013) 424-431.

[53] J.H. Ramirez, F.J. Maldonado-Hódar, A.F. Pérez-Cadenas, C. Moreno-Castilla, C.A. Costa, L.M. Madeira, Appl. Catal. B – Environ. 75 (2007) 312–323.

Table 1 - Textural characteristics of the fresh and used Fe-ZSM-5 catalyst obtained by N_2 adsorption.

Catalyst	S_{BET}	V_T	V_{meso}	W_0	L_0
	m^2/g	cm^3/g	cm^3/g	cm^3/g	nm
Fresh	320	0.237	0.113	0.124	0.63
Used pH= 1.5	237	0.208	0.119	0.089	0.83
Used pH= 2.0	290	0.222	0.108	0.114	0.76
Used pH= 2.5	311	0.236	0.115	0.121	0.68
Used pH= 3.0	305	0.232	0.111	0.121	0.63
Used pH= 4.0	320	0.236	0.112	0.124	0.60

Figures captions

Figure 1 - N_2-adsorption isotherms (a) and pore size distribution obtained by application of the DFT method (b) for fresh and used samples.

Figure 2 - SEM images of fresh (a, b) and used at pH= 1.5 (c) catalysts.

Figure 3 - Mapping of the distribution of the elements on the catalyst surface and chemical analysis obtained by SEM / EDS of (a) fresh catalyst, and (b) catalyst used at pH= 1.5

Figure 4 - Dye elimination in terms of decolorization and TOC removal at steady-state (a), and iron leaching from the catalyst support (b), by the heterogeneous Fenton in a CSTR in five consecutive runs (pH = 3, T = 50 ^{o}C, d_{p2}, $[H_2O_2]_{feed}$ = 6 mM, *W/Q* ratio = 60 mg.min/mL and t_{resid} = 30 min).

Figure 5 – Color and TOC removal at steady-state in the heterogeneous (with Fe/ZSM-5 zeolite) and in the homogeneous (with $Fe_2SO_4.7H_2O$) Fenton process in a CSTR (pH = 3, T = 50 ^{o}C, $[H_2O_2]_{feed}$ = 6 mM, d_{p2} and *W/Q* ratio $_{\text{in heterogeneous process}}$ = 60 mg.min/mL, $[Fe^{2+}]_{\text{in homogeneous process}}$ = 0.262 mg/L, and t_{resid} = 30 min).

Figure 6 - Effect of hydrogen peroxide feed concentration in color and TOC removals at steady-state (a) and iron leaching from the catalyst support (b) by the heterogeneous Fenton process in the CSTR (pH = 3, T = 50 ^{o}C, d_{p2}, *W/Q* ratio = 60 mg.min/mL and t_{resid} = 30 min).

Figure 7 - Effect of particle size in color and TOC removal at steady-state (a) and iron leaching from the catalyst support (b) by the heterogeneous Fenton' s reaction in a CSTR (pH = 3, $[H_2O_2]_{feed}$ = 6 mM, T = 50 ^{o}C, *W/Q* ratio = 60 mg.min/mL and t_{resid} = 30 min).

Figure 8 - Influence of pH in decolorization and TOC removal at steady-state (a) and iron leaching from the catalyst support (b) by the heterogeneous Fenton in a CSTR (T = 50 ^{o}C, d_{p2}, $[H_2O_2]_{feed}$ = 6 mM, *W/Q* ratio = 60 mg.min/mL and t_{resid} = 30 min).

Figure 9 - Influence of residence time in decolorization and TOC removal at steady-state (a) and iron leaching from the catalyst support (b) by the heterogeneous Fenton's oxidation in a CSTR (pH = 3, $[H_2O_2]_{feed}$ = 6 mM , T = 50 ^{o}C, d_{p2} and *W/Q* ratio = 60 mg.min/mL).

Figure 10 - Effect of contact time in decolorization and TOC removal at steady-state (a) and iron leaching from the catalyst support (b) by the heterogeneous Fenton in a CSTR (pH = 3, $[H_2O_2]_{feed}$ = 6 mM , T = 50 ºC, d_{p2}, t_{resid} = 30 min).

Figure 11 - Effect of the temperature in decolorization and TOC removal at steady-state (a) and iron leaching from the catalyst support (b) by the heterogeneous Fenton in a CSTR (pH = 3, $[H_2O_2]_{feed}$ = 6 mM, d_{p2}, *W/Q* ratio = 60 mg.min/mL and t_{resid} = 30 min).

Figure 12 – Experimental and model OII dye removal as a function of contact time (a), Arrhenius law linearization (b) and experimental and model OII dye removal as a function of temperature (c). For the experimental conditions, please refer to previous figures.

Figure 13 - Specific oxygen uptake rate along time in the run with optimized parameters (pH = 3, T = 70 ºC, d_{p2}, $[H_2O_2]_{feed}$ = 6 mM, *W/Q* = 200 mg.min/mL and t_{resid} = 90 min).

Figure 1

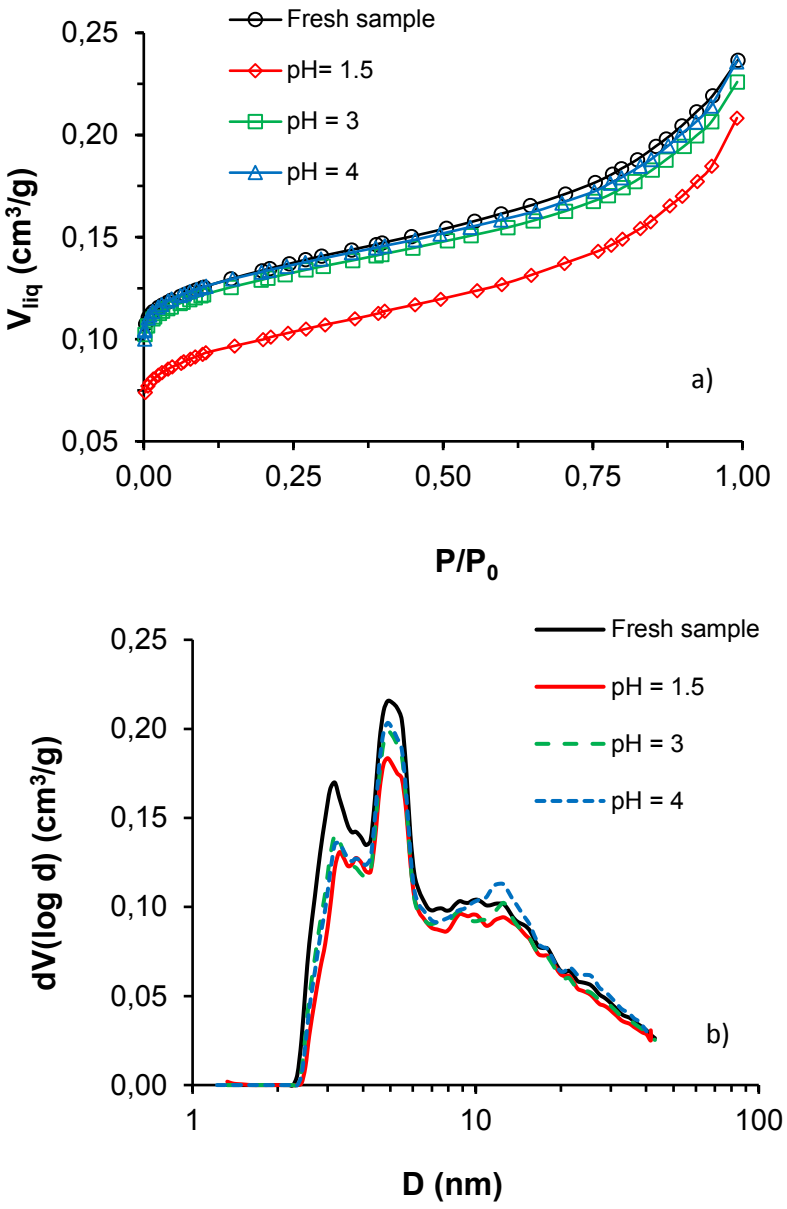
Fresh sample
pH= 1.5
pH = 3
pH = 4
0,25
0,20
0,15
0,10
0,05
V_{liq} (cm³/g)
a)
0,00
0,25
0,50
0,75
1,00
P/P0
Fresh sample
pH = 1.5
pH = 3
pH = 4
dV(log d) (cm³/g)
0,25
0,20
0,15
0,10
0,05
0,00
b)
1
10
100
D (nm)

Figure 2

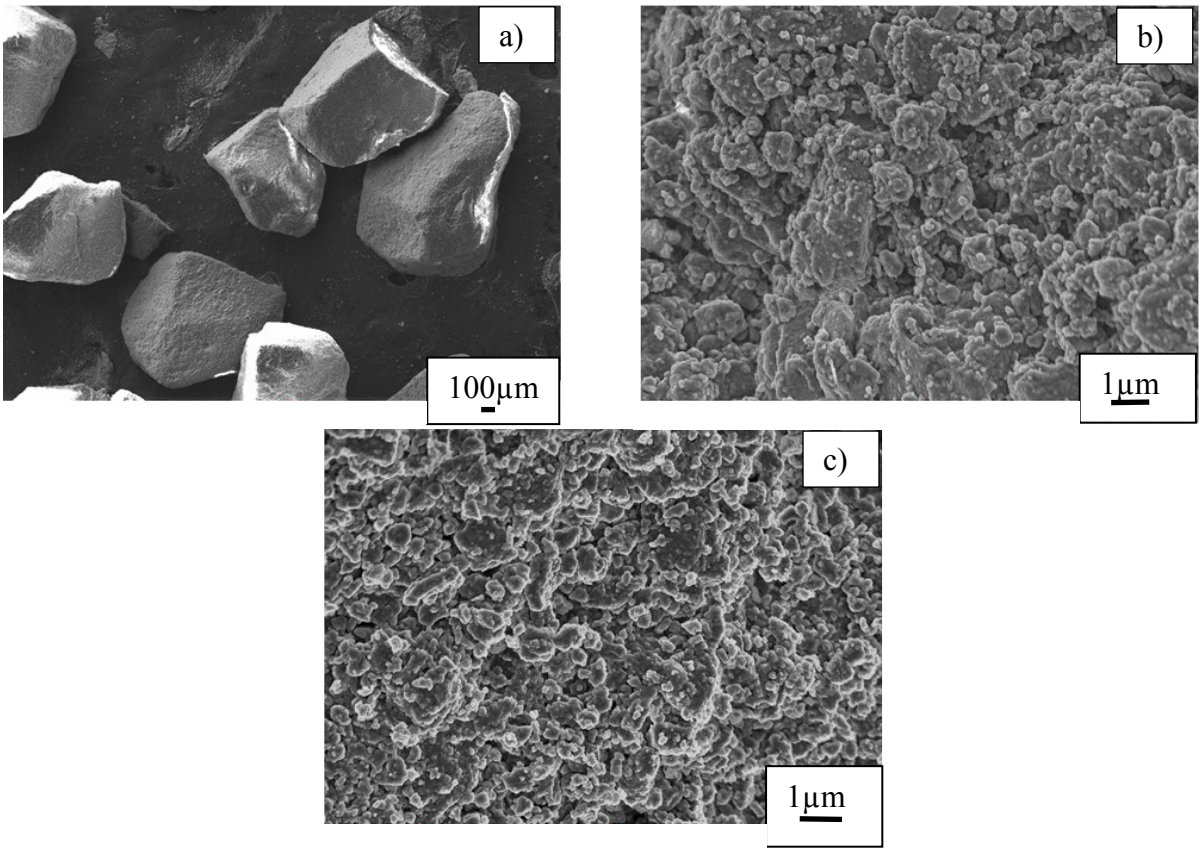

Figure 3

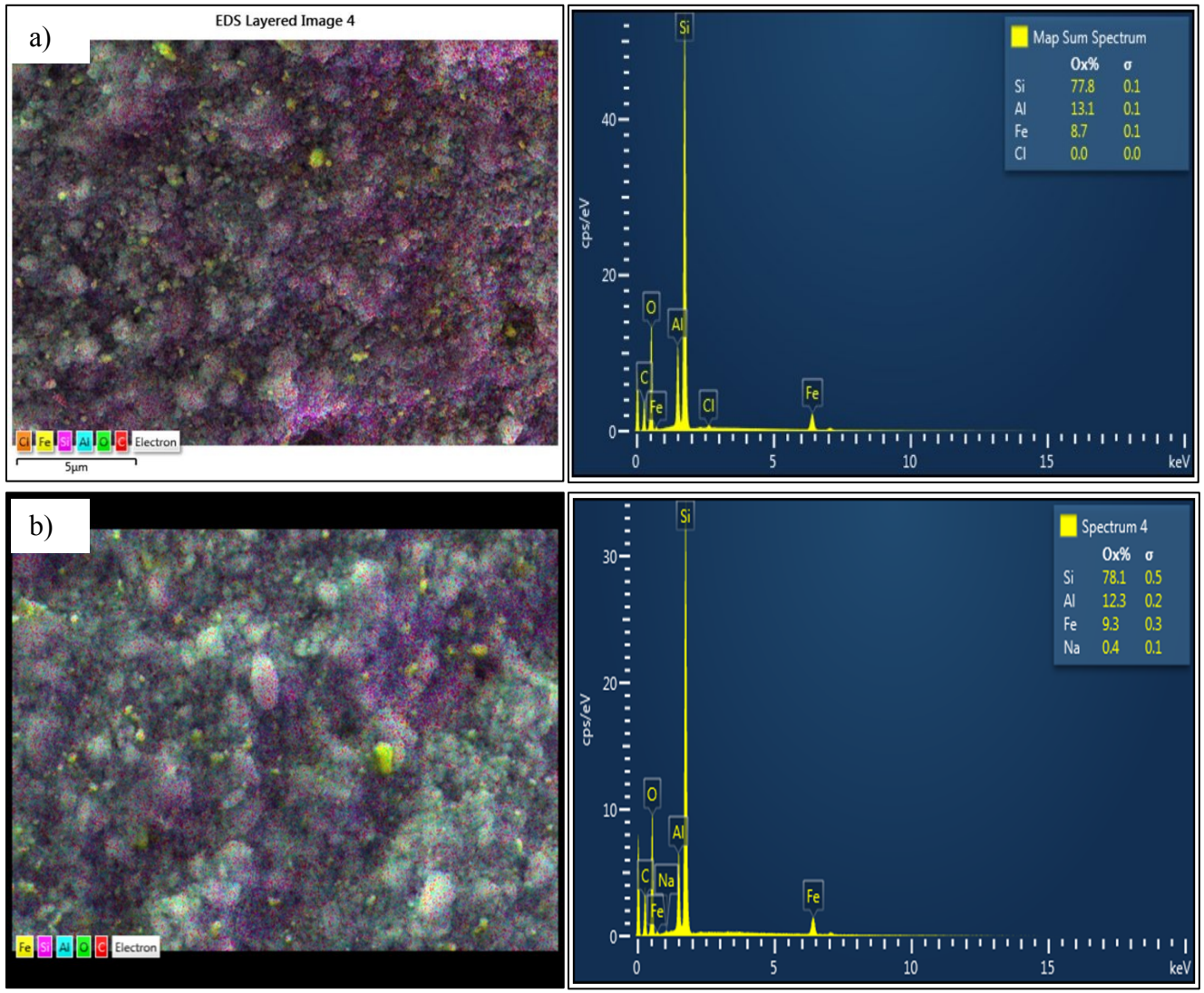
a)
EDS Layered Image 4
Cl Fe Si Al O C Electron
5µm
Si
O
Al
C
Fe
Cl
Fe
cps/eV
keV
Map Sum Spectrum
Ox% σ
Si 77.8 0.1
Al 13.1 0.1
Fe 8.7 0.1
Cl 0.0 0.0
b)
Fe Si Al O C Electron
Si
O
Al
C
Na
Fe
Fe
cps/eV
keV
Spectrum 4
Ox% σ
Si 78.1 0.5
Al 12.3 0.2
Fe 9.3 0.3
Na 0.4 0.1

Figure 4

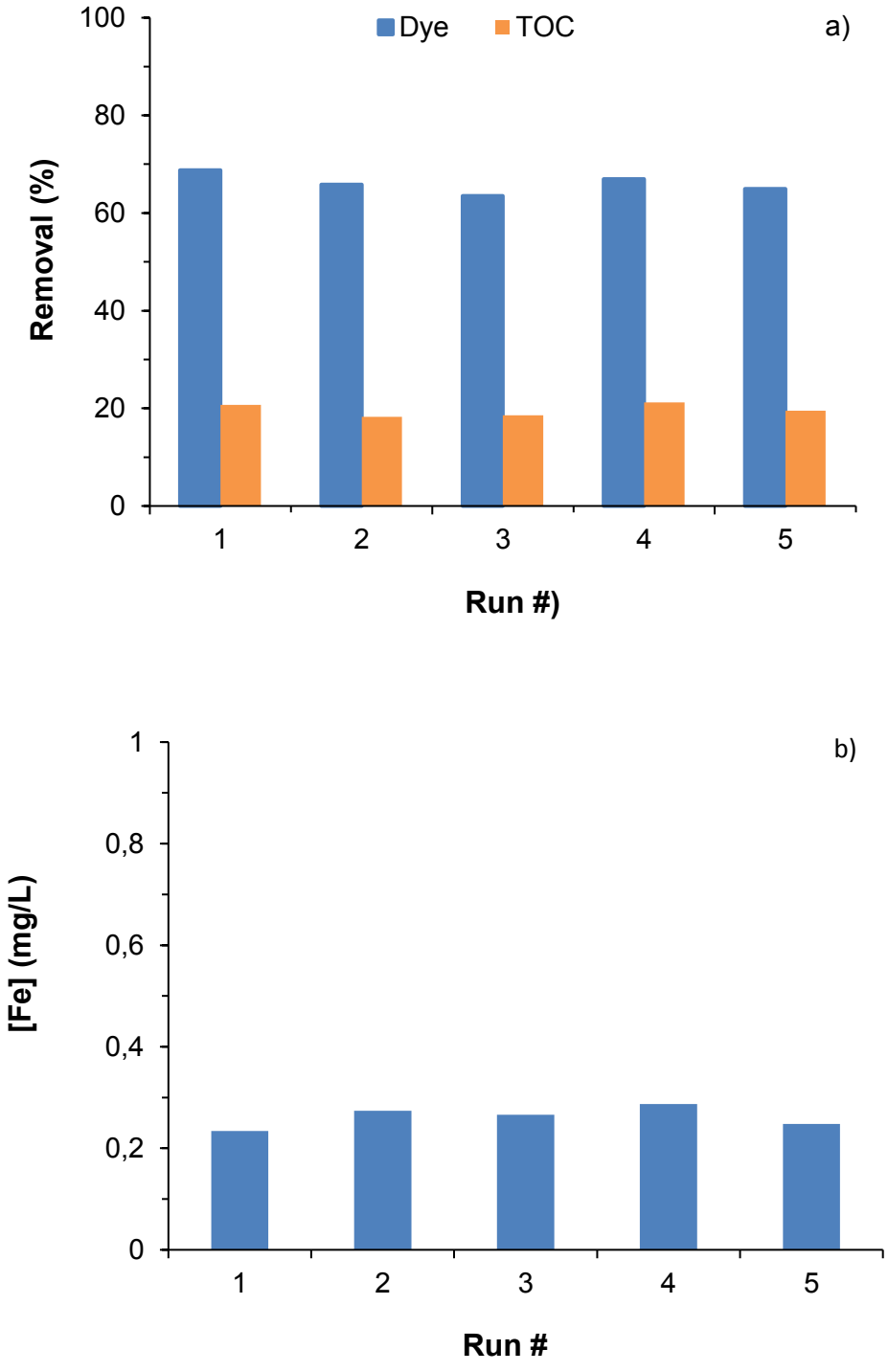
Dye
TOC
a)
Removal (%)
100
80
60
40
20
0
1
2
3
4
5
Run #)
b)
[Fe] (mg/L)
1
0,8
0,6
0,4
0,2
0
1
2
3
4
5
Run #

Figure 5

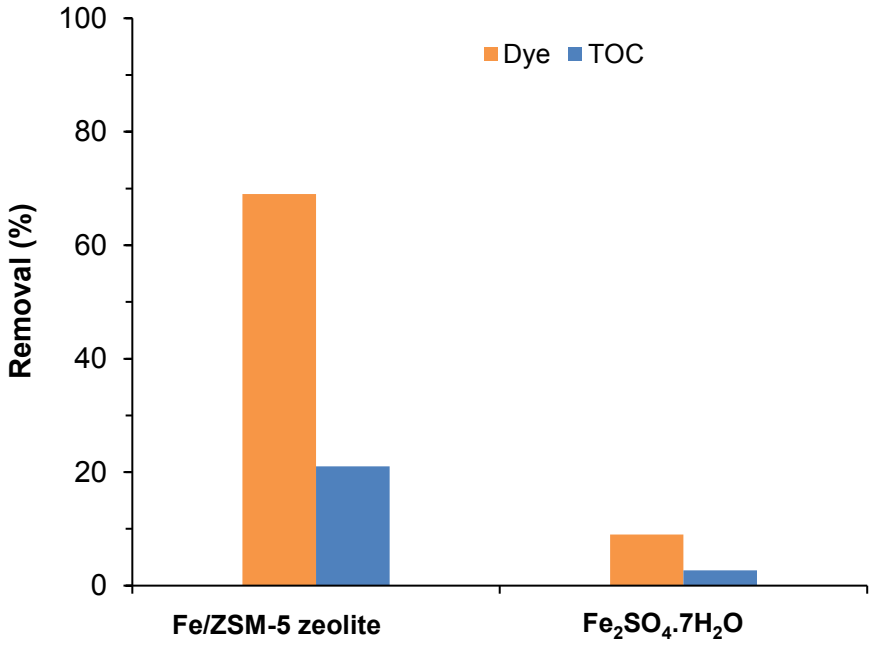

Figure 6

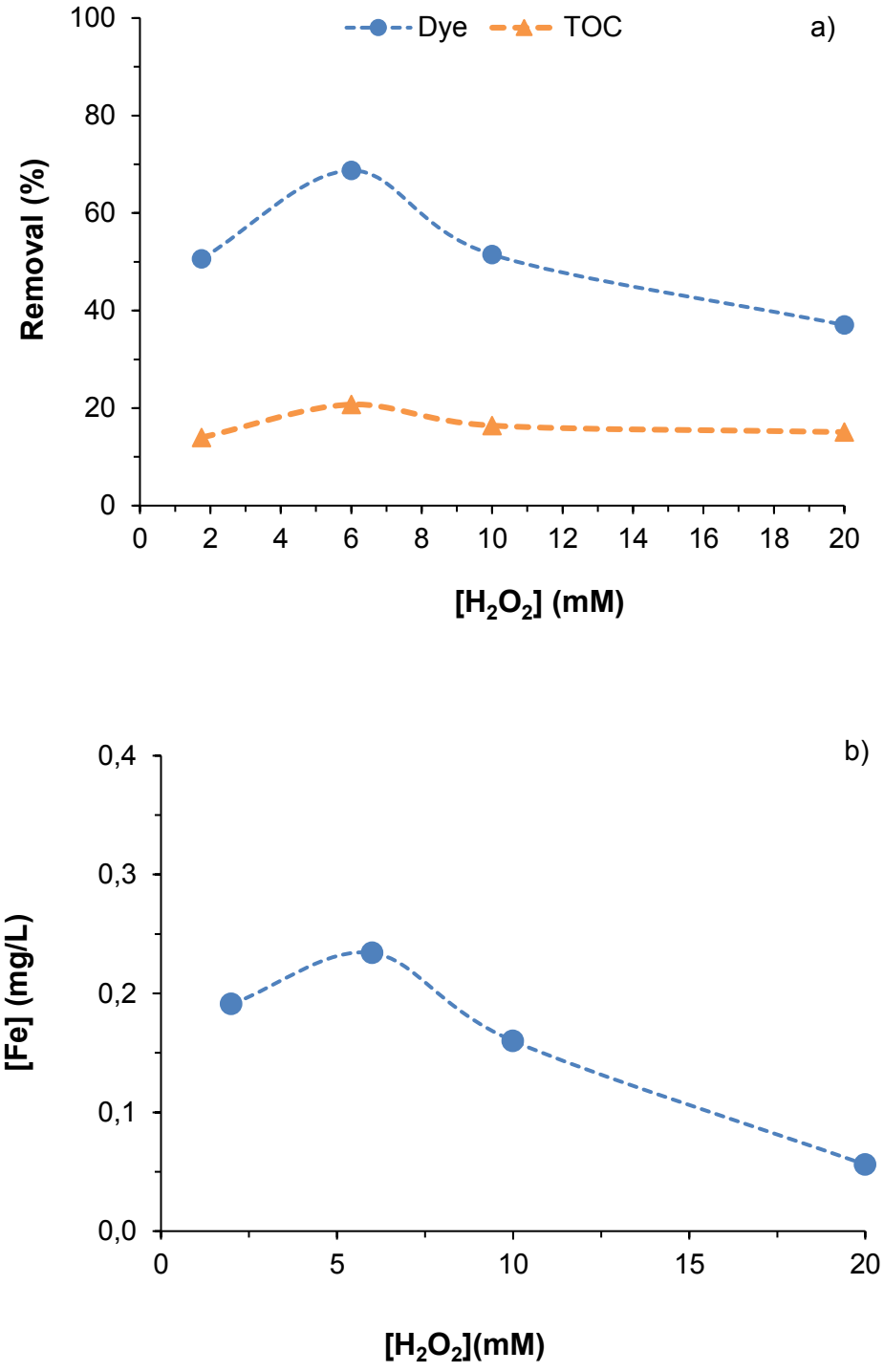
Dye
TOC
a)
Removal (%)
100
80
60
40
20
0
0
2
4
6
8
10
12
14
16
18
20
[H2O2] (mM)
b)
[Fe] (mg/L)
0,4
0,3
0,2
0,1
0,0
0
5
10
15
20
[H2O2](mM)

Figure 7

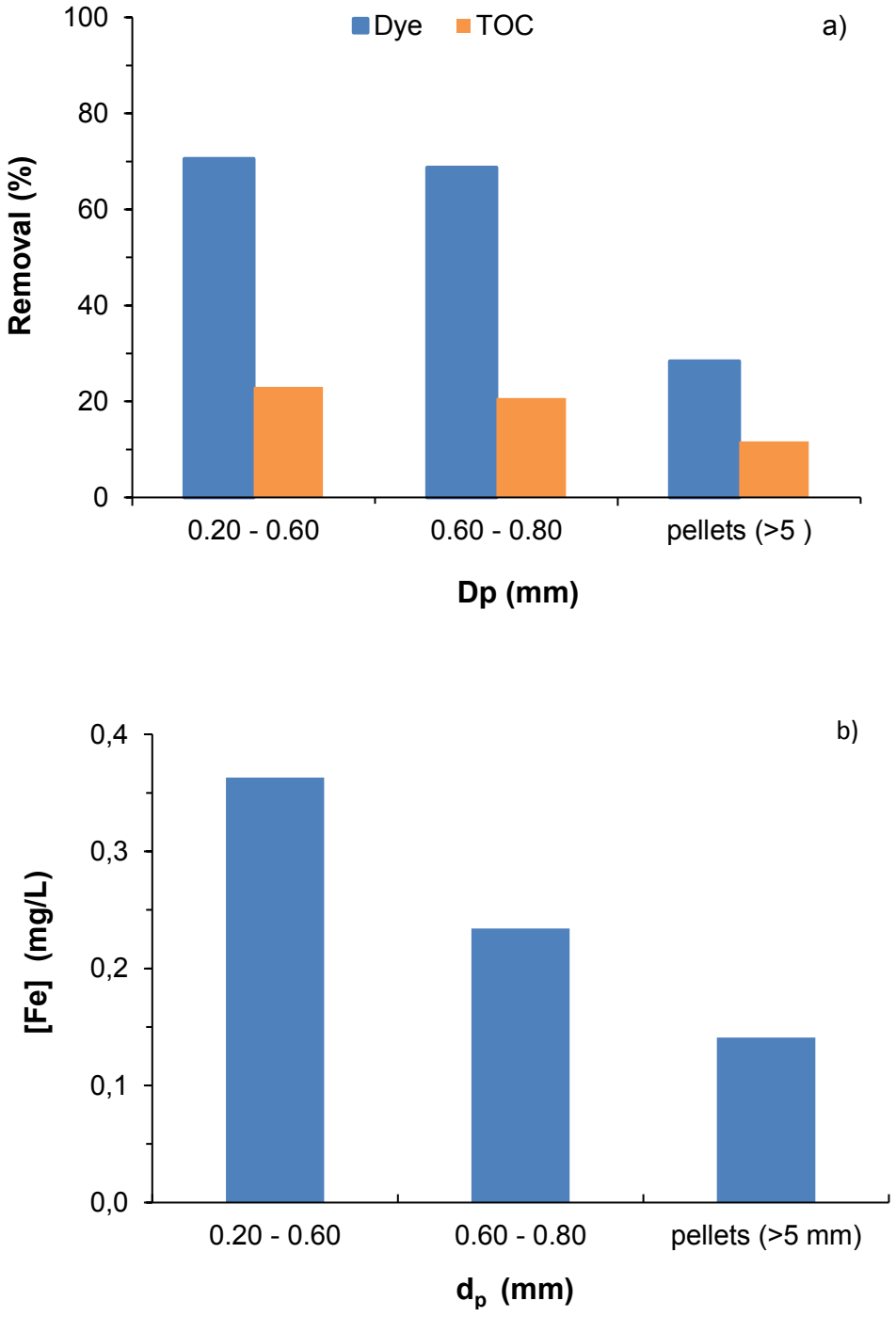
a)
Dye
TOC
100
80
60
40
20
0
Removal (%)
0.20 - 0.60
0.60 - 0.80
pellets (>5)
Dp (mm)
b)
0,4
0,3
0,2
0,1
0,0
[Fe] (mg/L)
0.20 - 0.60
0.60 - 0.80
pellets (>5 mm)
d_p (mm)

Figure 8

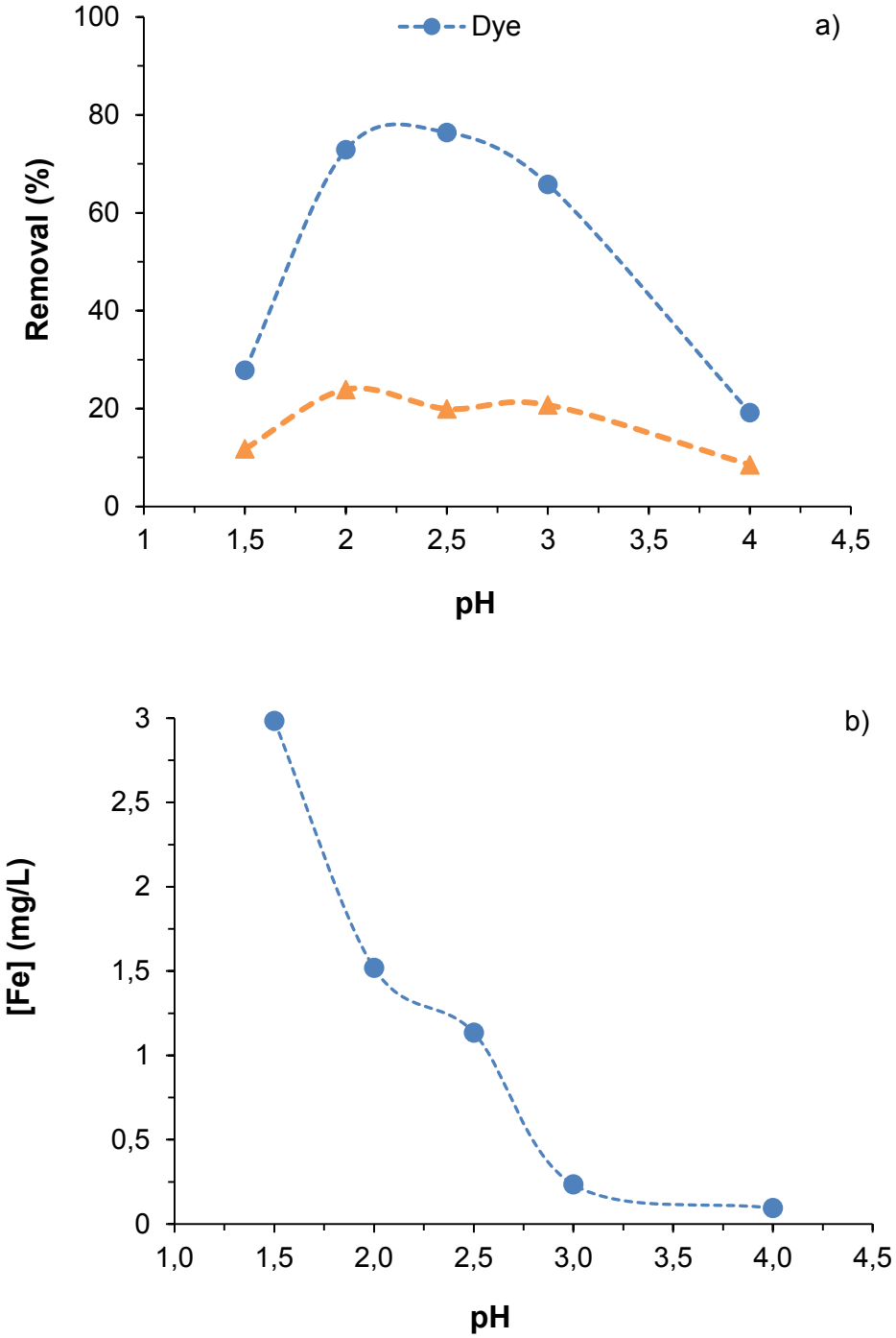
Dye
a)
Removal (%)
100
80
60
40
20
0
1
1,5
2
2,5
3
3,5
4
4,5
pH
b)
[Fe] (mg/L)
3
2,5
2
1,5
1
0,5
0
1,0
1,5
2,0
2,5
3,0
3,5
4,0
4,5
pH

Figure 9

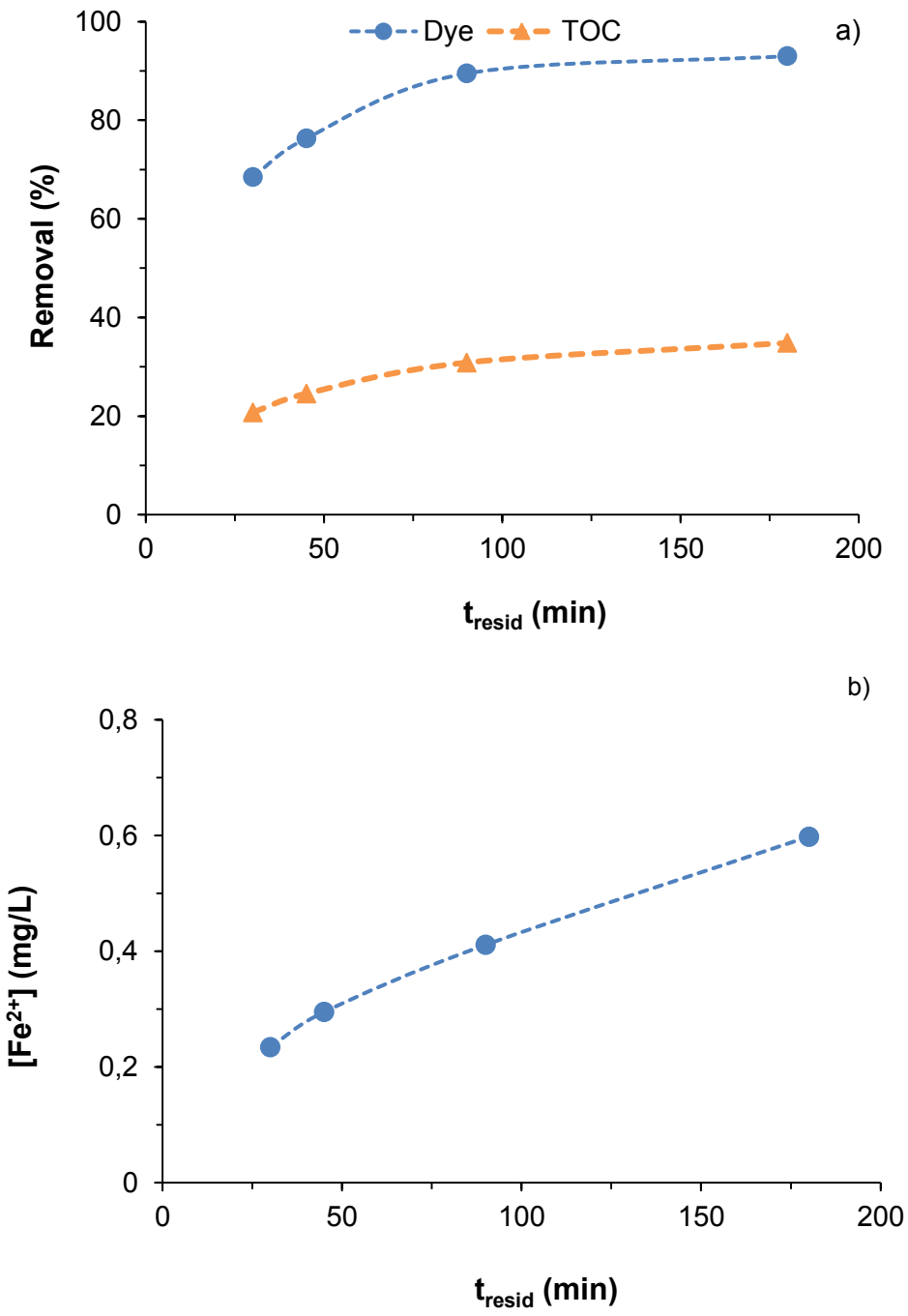
Dye
TOC
a)
Removal (%)
100
80
60
40
20
0
0
50
100
150
200
t_{resid} (min)
b)
$[Fe^{2+}]$ (mg/L)
0,8
0,6
0,4
0,2
0
0
50
100
150
200
t_{resid} (min)

Figure 10

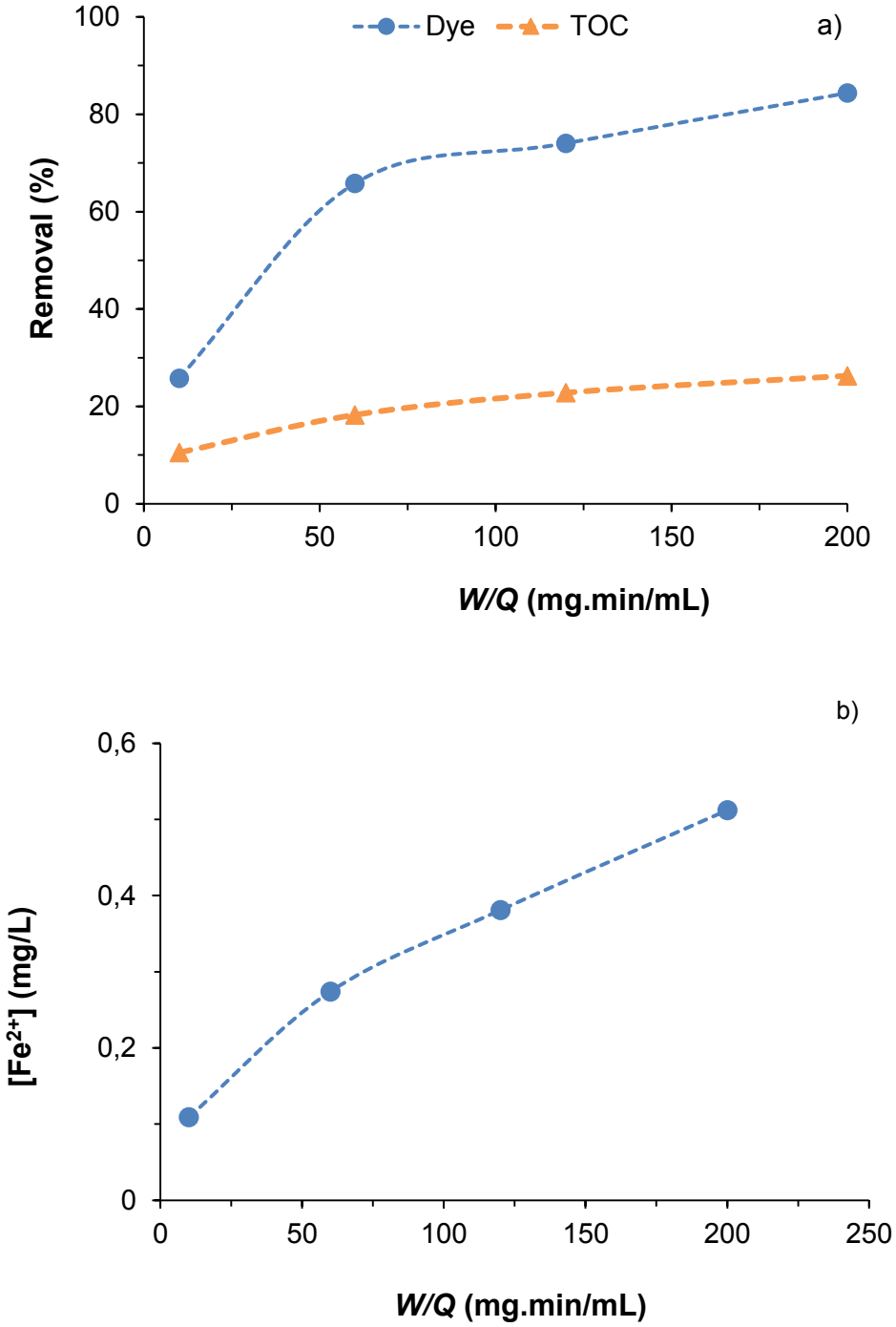
Dye
TOC
a)
Removal (%)
100
80
60
40
20
0
0
50
100
150
200
W/Q (mg.min/mL)
b)
[Fe2+] (mg/L)
0,6
0,4
0,2
0
0
50
100
150
200
250
W/Q (mg.min/mL)

Figure 11

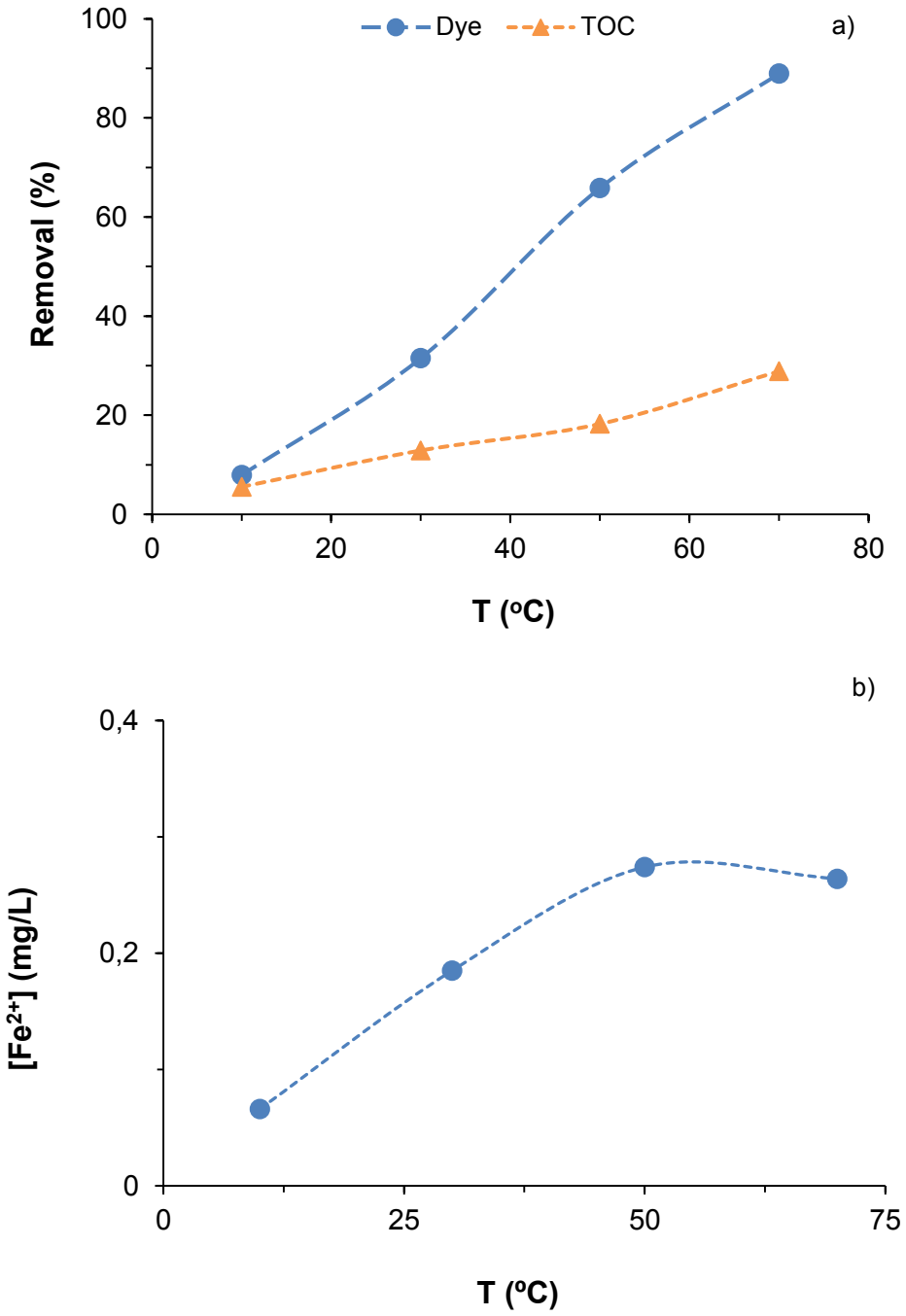
a)
Dye
TOC
Removal (%)
100
80
60
40
20
0
0
20
40
60
80
T (ºC)
b)
[Fe2+] (mg/L)
0,4
0,2
0
0
25
50
75
T (ºC)

Figure 12

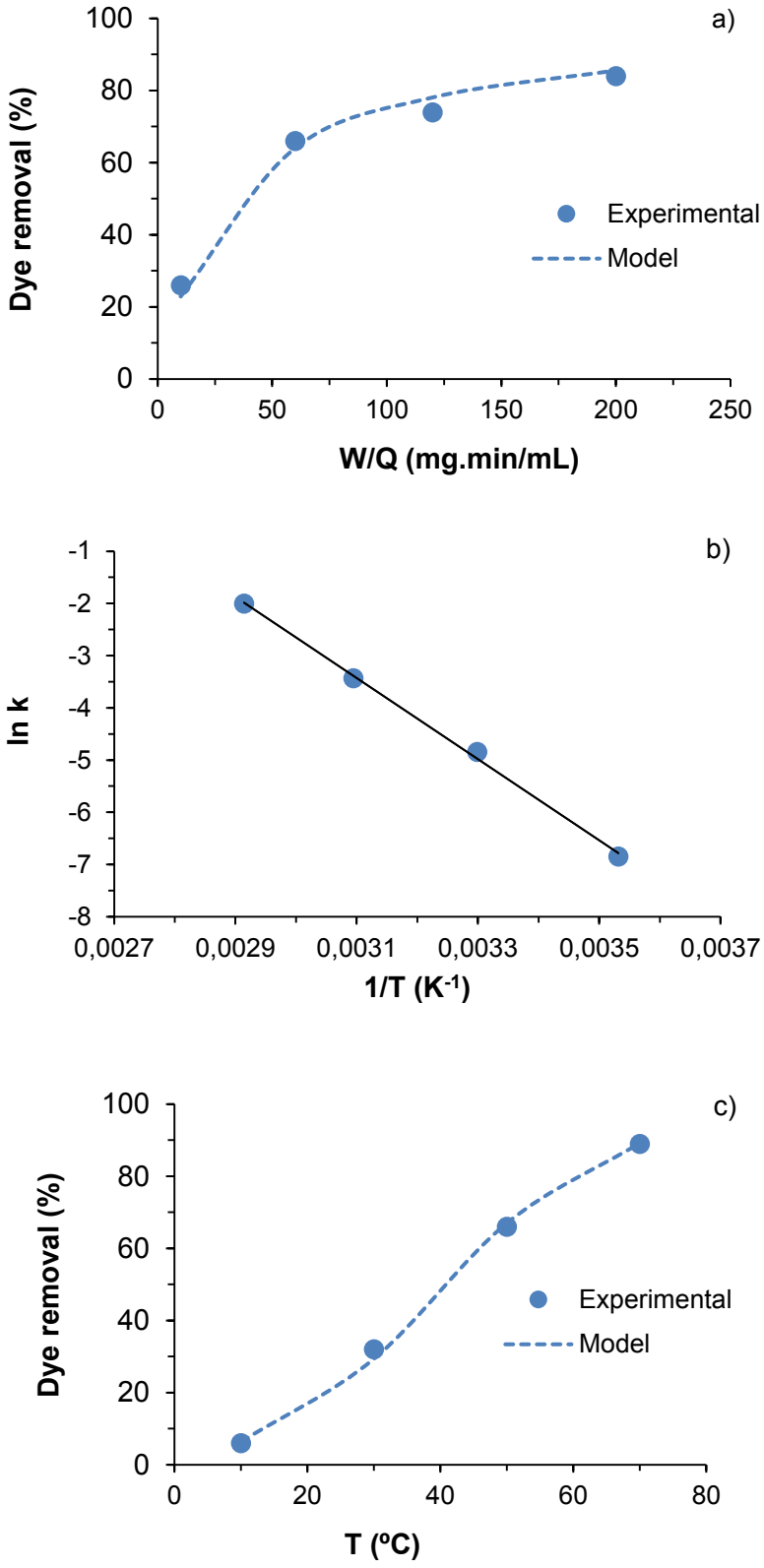
a)
Dye removal (%)
100
80
60
40
20
0
0
50
100
150
200
250
W/Q (mg.min/mL)
Experimental
Model
b)
ln k
-1
-2
-3
-4
-5
-6
-7
-8
0,0027
0,0029
0,0031
0,0033
0,0035
0,0037
1/T (K-1)
c)
Dye removal (%)
100
80
60
40
20
0
0
20
40
60
80
T (ºC)
Experimental
Model

Figure 13